Talanta 85 (2011) 1174–1179

Contents lists available at ScienceDirect

Talanta

journal homepage: www.elsevier.com/locate/talanta

Bio-electrocatalysis of NADH and ethanol based on graphene sheets modified electrodes

Kai Guo[a,1], Kun Qian[b,1], Song Zhang[a], Jilie Kong[a], Chengzhong Yu[b,*], Baohong Liu[a,**]

[a] Department of Chemistry and Key Lab of Molecular Engineering of Polymers of Chinese Ministry of Education, Fudan University, Shanghai 200433, PR China
[b] ARC Centre of Excellence for Functional Nanomaterials and Australian Institute for Bioengineering and Nanotechnology, The University of Queensland, Brisbane, QLD 4072, Australia

ARTICLE INFO

Article history:
Received 22 February 2011
Received in revised form 10 May 2011
Accepted 19 May 2011
Available online 27 May 2011

Keyword:
Graphene
Alcohol dehydrogenase
NADH
Ethanol biosensor

ABSTRACT

Characterization and application of graphene sheets modified glassy carbon electrodes (graphene/GC) have been presented for the electrochemical bio-sensing. A probe molecule, potassium ferricyanide is employed to study the electrochemical response at the graphene/GC electrode, which shows better electron transfer than graphite modified (graphite/GC) and bare glassy carbon (GC) electrodes. Based on the highly enhanced electrochemical activity of NADH, alcohol dehydrogenase (ADH) is immobilized on the graphene modified electrode and displays a more desirable analytical performance in the detection of ethanol, compared with graphite/GC or GC based bio-electrodes. It also exhibits good performance of ethanol detection in the real samples. From the results of electrochemical investigation, graphene sheets with a favorable electrochemical activity could be an advanced carbon electrode materials for the design of electrochemical sensors and biosensors.

1. Introduction

Ethanol is the most common poisonous substance involved in medical-legal cases and it frequently results in a variety of traffic accidents. Thus the accurate measurement of ethanol concentration is very important for medicine study and lawsuit cases. Various approaches have been proposed to meet the rising demands for ethanol detection [1–4]. These methods usually suffered from series of problems, e.g. expensive instruments, time-consuming process and sophisticated operation procedures. Currently the electrochemical biosensors, because of their inexpensive, rapid, reliable and specific characteristics, have made substantial progress in the area of ethanol sensing [5,6]. The enzymes normally used in the developed electrochemical biosensors for ethanol detection are alcohol oxidase (AOD) or alcohol dehydrogenase (ADH). Generally, in an ADH based electrochemical biosensor, β-nicotinamide adenine dinucleotide (NADH) is always involved as a cofactor during the detection of ethanol, which has attracted considerable attention [7]. However, the electro-oxidation of NADH at a conventional electrode takes place at considerable over-potentials, greater than 0.6 V (vs. Ag/AgCl) [8]. This over-potential oxidation may lead to oxidation of other electro-active species present in the solutions and interfere with the target analysis [9].

In order to solve these problems, many compounds [10–13] have been modified on the electrode surface as electron-transfer mediators to catalyze the oxidation of NADH and fabricate the electrochemical sensors. However, due to the slower diffusion of NADH within the immobilized mediators or redox self-exchange limitation within the film, the electrochemical biosensors usually displayed relatively low sensitivity. In recent years, carbon based nanomaterials, owning to their chemical inertness, relatively wide potential window, low background current and suitability for different types of analysis, have been devoted to constructing series of biosensors [14,15] and decreasing the high over-potential for NADH electro-oxidation through improving the electron-transfer kinetics and minimizing the surface fouling [16–18].

Among these carbon nanomaterials, graphene [19], which is a two-dimensional monolayer of carbon atoms parked into a dense hexagonal network structure, has received considerable attention from both the experimental and theoretical scientific communities in the last several years [20]. Because of its unique electric, thermal and mechanical properties [21], graphene has provided strong potentials in synthesizing nanocomposites [22–24] and fabricating micro-electrical devices and biosensors [24,25]. Fan et al. reported that graphene oxide could not only facilitate electron transfer but also keep the bioactivity of metalloproteins at electrode surface [26]. Recently, Zhou et al. had established electrochemical platform based on chemo-reduced graphene oxide obtained from a modified Hummers method [27] and Shan et al. observed that these

* Corresponding author. Fax: +86 21 6564 1740.
** Corresponding author. Tel.: +86 21 6564 2405; fax: +86 21 6564 1740.
E-mail addresses: c.yu@uq.edu.au (C. Yu), bhliu@fudan.edu.cn (B. Liu).
[1] These authors contributed equally to this work.

0039-9140/$ – see front matter © 2011 Elsevier B.V. All rights reserved.
doi:10.1016/j.talanta.2011.05.038

graphene materials displayed enhanced properties when functionalized by ionic liquids [28]. Therefore, the design and construction of this kind of materials for electrode modification are becoming important aspects for improving properties of the electrochemical biosensors.

In this research, the graphene sheets modified glassy carbon electrode has been developed for electrochemical sensing of NADH and ethanol. The advantages of graphene modified electrodes are studied by the comparison with the conventional graphite functionalized and bare glassy carbon electrodes for the electrochemical characterization and applications of NADH sensing. The electrochemical behavior of electro-active compound at the graphene/GC showed an increase of electron transfer rate compared with graphite modified and bare GC electrodes. Additionally, based on the better electro-catalytic activity of NADH, the joint application of graphene and alcohol dehydrogenase (ADH) gave rise to an ethanol biosensor with high selectivity and sensitivity in a wide range of detection.

2. Experimental

2.1. Reagents

ADH (E.C. 1.1.1.1, 340 U mg^{-1}, from *Saccharomyces cerevisiae*), bovine serum albumin (BSA), β-nicotinamide adenine dinucleotide (NAD^+) were purchased from Sigma. Graphite and hydrazine were purchased from Aldrich. Nicotinamide adenine dinucleotide (oxidized state, NADH) and glutaraldehyde were obtained from Fluka. All other chemicals were analytical grade and used without further purification. All solutions were prepared with ultrapure water.

2.2. Synthesis of materials

Graphite oxide (GO) was prepared according to the Staudenmaier method [29]. A reaction flask containing a mixture of sulfuric acid (175 mL) and nitric acid (90 mL) and cooled by immersion in an ice bath. The acid mixture was stirred and allowed to cool for 30 min, and graphite (10 g) was added under vigorous stirring to avoid agglomeration. After the graphite powder was well dispersed, potassium chlorate (110 g) was added slowly over 30 min to avoid sudden increases in temperature. The reaction flask was loosely capped to allow evolution of gas from the reaction mixture and allowed to stir for 5 days at room temperature. On completion of the reaction, the mixture was poured into 10 L of deionized water and filtered. The GO was redispersed and washed in a 5% solution of HCl. The GO was then washed repeatedly with deionized water until the pH of the filtrate was neutral. The GO slurry was dried at 60 °C. Over 10 g of graphite oxide can be produced using the modified Staudenmaier method. The obtained graphite oxide (0.2 g) dispersed in 500 mL deionized water was exfoliated to graphene oxide under ultrasonic treatment for 1 h. The resulting homogeneous dispersion (10 mL, containing 4 mg graphite oxide) was mixed with 10 mL of water, 10 mg of hydrazine solution (35 wt% in water, containing 2.8 mg hydrazine) and 35.0 μL of ammonia solution (28 wt% in water) [20,30]. After being vigorously stirred for 30 min, a water bath (95 °C) is launched for 1 h. The resulting mixture was filtered and washed to get the final graphene.

2.3. Characterizations of materials

X-ray diffraction (XRD) patterns were recorded on the German Bruker D8 advanced X-ray diffracto-meter using the Ni-filtered Cu KR radiation with a wavelength of 0.154 nm (40 mV working voltage and 40 mA working current). The samples were first pressed and then loaded onto the sample plate. The resulting XRD patterns were recorded and analyzed by the Bruker software DIFFRAC-XRD Commander. TEM images were directly obtained on the graphene deposited Cu grid with a JEOL 2011 microscope operated at 200 kV. SEM micrographs were taken with a Philips XL30 microscope operated at 20 kV and no coating procedures were employed. The reduced graphene was sonicated and then deposited on the sample carrier before SEM observation. XPS measurements were performed using a RBD upgraded PHI-5000C ESCS system (Perkin Elemer) with Al Kα radiation ($h\nu$ = 1486.6 eV).

2.4. Electrode preparation and modification

Glass carbon electrode (GC, 3 mm diameter) was polished with 1, 0.3 and 0.05 μm alumina powder sequentially and then washed with ultrasonication in water and ethanol for 3 min, respectively. The clean GC electrode was dried at ambient condition. The modifications of graphene and graphite were carried out by pipetting an aliquot of 6 μL their DMF suspensions (5 mg mL^{-1}) uniformly onto the glass carbon electrode surface. The modified electrodes were then dried under ambient condition for 2 h.

For fabricating ADH-based bio-electrodes, a 1 wt% aqueous solution of BSA and ADH at given concentrations was mixed with the volume ratio of 1:2 to give an ADH-BSA mixture, and 8 μL of the resulting mixture was coated onto the electrodes. A 2 μL aqueous solution of glutaraldehyde (40 mM) was further pipetted onto electrodes to cross-link the ADH and 3 μL Nafion polymer (0.5 wt%) was dropped at last onto the electrodes. The prepared electrodes were air-dried, rinsed with deionized water and used as ADH/graphene/GC, ADH/graphite/GC and ADH/GC electrode.

After the modification, graphene, graphite and bare GC based modified electrodes were stored in 0.1 M pH 7.4 phosphate buffer solution (PBS) for 30 min before the measurement and kept in 0.1 M pH 7.4 PBS at 4 °C when not in use. The real samples were diluted with 0.1 M pH 7.4 PBS in appropriate concentration and used without other pretreatment.

All electrochemical measurements were carried out at a CHI 660C electrochemical workstation (Chenhua Instrument Co. Shanghai, China) assembled with three-electrode system.

3. Results and discussion

3.1. Characterization of graphene

The graphene used here is prepared using the reported oxidation–reduction method based on the graphite oxide [20], which is easily obtained after acid oxidation of normal graphite via the modified Staudenmaier method [29]. The resulting graphite oxides are exfoliated to graphene oxides by ultrasonic dispersion [31]. The obtained graphene oxides are finally reduced to graphene by hydrazine [30]. In a manner that parallels previous results [20], a monolayer structure of graphene is observed through the atomic force microscope (AFM) with a height profile plot showing the thickness less than 1 nm shown in Fig. S1A. The scanning electron microscope (SEM) and TEM images (Fig. S1B and C) also display the very thin layer of graphene.

The X-ray diffraction (XRD) patterns in Fig. 1 show that a typical spectrum of graphite phased carbon with a very sharp peak at $2\theta = 26.6°$, which corresponds to the diffraction of (0 0 2) plane, being the interlayer distance of $d_{002} = 0.336$ nm. A typical oxidation yields the appearance of diffraction peak of the graphite oxide at $2\theta = 14.2°$ without the peak of d_{002} visible in graphite due to the insertion of carboxyl groups to the graphite layers [29,32]. In the case of graphene and graphene oxide, no peaks can be observed, indicating a complete exfoliation of the original multilayered structure in graphite and graphite oxide [29].

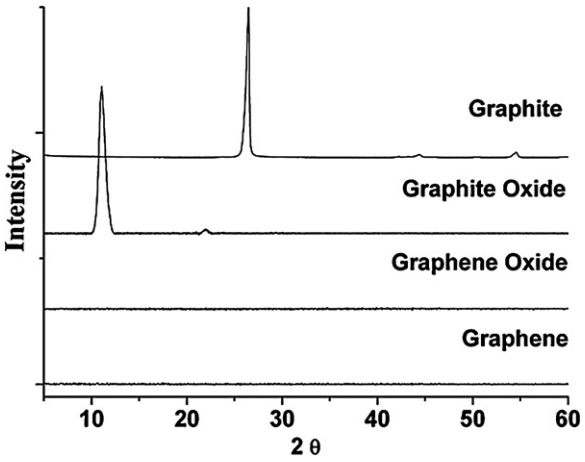

Fig. 1. XRD patterns of graphite, graphite oxide, graphene oxide and graphene.

In order to further confirm the reduction process, we employed XPS analysis for the graphite oxide and graphene obtained. As shown in Fig. 2, the graphite oxide/graphene materials contained O and C with the chemical binding energies of O 1s (~530 eV) and C 1s (~280 eV) respectively, according to the XPS survey spectrum [33,34]. It is observed the O content decreased significantly in the case of graphene compared to the graphite oxide, indicating that chemo-reduction has been well performed and graphene have been successfully synthesized with low content of oxygen.

3.2. Electrochemical characterization of the graphene/GC electrode

$[Fe(CN)_6]^{3-/4-}$ couple is widely used as an electrochemical probe to investigate the properties of the modified electrodes. Fig. 3A shows the voltammetric response of $[Fe(CN)_6]^{3-/4-}$ at the bare GC, graphite and graphene modified electrodes. The bare GC electrode gives the reversible electrochemical response for the probe. Compared with the bare electrode, cyclic voltammograms of the graphite modified electrodes show less reversible response due to the weaker conductivity of graphite assembled layers. However, after functionalized with graphene, the peak-to-peak potential difference is similar as the bare electrode, indicating that the well-defined graphene film possesses the essential surface structure and electronic properties to support the rapid electron transfer in this redox system. Fig. 3B shows CVs of graphene, graphite and bare GC electrodes in 0.1 M pH 7.0 phosphate buffer solutions acquired at a

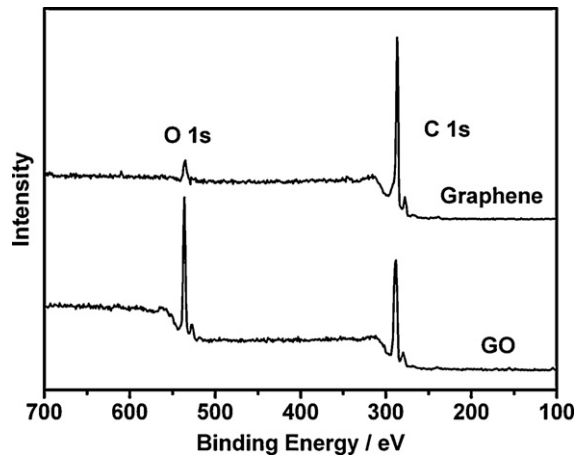

Fig. 2. XPS spectra of graphite oxide and graphene.

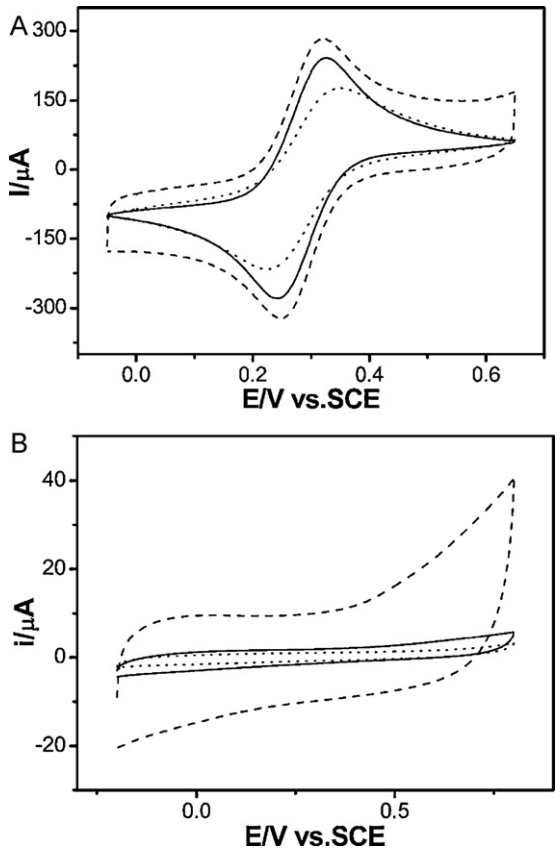

Fig. 3. (A) Cyclic voltammograms for GC (solid line), graphite (dot line) and graphene (dash line) modified GC electrodes in 10 mM $[Fe(CN)_6]^{3-}$ with 2 M KCl as electrolyte at a scan rate of 50 mV s^{-1}, and (B) 0.1 M pH 7.0 PBS between −0.2 V and 0.8 V. Scan rate: 50 mV s^{-1}.

scan rate of 50 mV s^{-1}. From the double layer capacitance of all the electrodes, the graphene modified electrode displays the highest charging current, indicating an expanded electrochemical active surface area on the modified electrode [35]. According to Eq. (1) [36]:

$$Q = (2nFAD_o^{1/2}\pi^{-1/2}C_o)t^{1/2} \quad (1)$$

where Q is the absolute value of the reduction charge, n is the number of electrons for the reaction, F is the Faraday constant, A is the apparent electrode area, D_o is the diffusion coefficient of the oxidized form, hexacyanoferrate ($D_o = 1.183 \times 10^{-5}$ cm^2 s^{-1}), C_o is the bulk concentration of the oxidized form (C_o = 10 mM), and t is the time [32]. From the slop of the Q–$t^{1/2}$ line, the sequence of values of A for the different electrodes is graphene/GC (0.127 cm^2) > bare GC (0.092 cm^2) > graphite/GC (0.074 cm^2). The larger value of apparent electrode area (A) can be observed at graphene functionalized electrode and might be a promising material for electrochemical sensing applications.

3.3. Electrocatalytic oxidation of NADH on the graphene/GC electrodes

In order to make a further understanding towards the electrochemical properties of graphene, the electro-oxidation of nicotinamide adenine dinucleotide hydrate (NADH), which has received intensive interest for the development of amperometric biosensors and bio-electronic devices associated with NAD^+-dehydrogenase [7,37] was also investigated. Fig. 4A shows the comparison of CVs of 5 mM NADH at different electrodes. The electro-oxidation exhibits an irreversible anodic peak at 0.64 V on

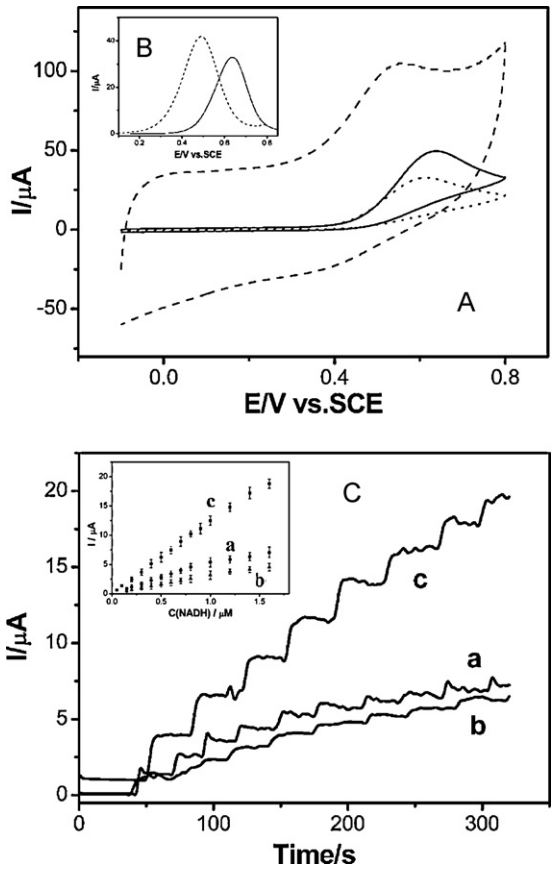

Fig. 4. (A) CVs of 5 mM NADH at graphene/GC (dash line), graphite/GC (dot line) and bare GC (solid line) electrodes in 0.1 M pH 7.0 PBS. Scan rate: 50 mV s^{-1}. (B) DPV for 5 mM NADH at graphene/GC (dash line) and bare GC (solid line) electrodes in 0.1 M pH 7.0 PBS. Conditions: Incr E, 4 mV; amplitude, 50 mV; pulse width, 50 ms; pulse period, 200 ms. (C) Current–time response curves for bare GC (at 0.65 V, line a), graphite/GC (at 0.65 V, line b) and graphene/GC (at 0.5 V, line c) electrodes with successive addition of NADH in stirred 0.1 M pH 7.0 PBS solution. Inset: calibration curves for NADH at bare GC (a), graphite/GC (b) and graphene/GC (c) electrodes.

the bare GC electrode. At the graphite/GC electrode, a decreased peak current suggests graphite modified layers partly blocked the electron transfer between NADH and the electrode surface. In the case of graphene/GC electrode, the anodic potential of NADH in pH 7.0 PBS shifts negatively to 0.5 V with an increased current signal in comparison with the bare and graphite modified electrodes. This peak potential for NADH at the graphene/GC is quite similar to the results obtained from the carbon nanotube functionalized electrode under the same condition [38].

The voltammetric behavior of graphene/GC electrode in NADH solution was further studied by differential pulse voltammetry (DPV) in the presence of 5 mM NADH as shown in Fig. 4B. In contrast to bare GC electrodes, the peak potential is negatively shifted from 0.64 V to 0.5 V when the electrode is modified by the graphene layer. There is no peak at 0.5 V in the absence of NADH. Therefore, the peak current at 0.5 V can be assigned to electro-catalytic oxidation of NADH by modified graphene at GC electrode. Compared with bare and graphite GC electrodes, the electro-oxidation current of NADH increased 20% and 50%, respectively. These results indicate that the presence of graphene films makes the electron transfer much easier, which may provide more favorable sites for bio-molecules and would be beneficial for accelerating electron transfer between the electrode and the species in solution.

To evaluate the analytical performance of the graphene/GC electrodes, the amperometric response towards the oxidation of NADH at graphene/GC was also recorded at 0.5 V with successive addition

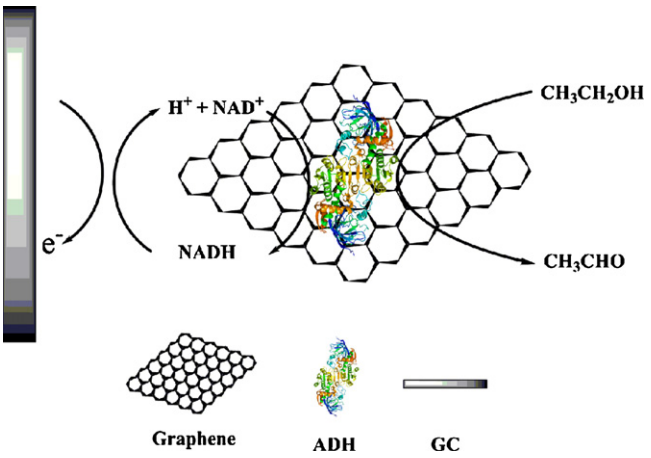

Fig. 5. Scheme of bio-electrocatalysis of ethanol on ADH/graphene modified glass carbon electrode.

of NADH (Fig. 4C). Well-defined steady state current were obtained at graphene/GC electrode, and the currents increased step wisely with successive additions of NADH. The response time (reaching 90% of maximum response) was less than 10 s indicating a fast process and well catalytic oxidation of NADH by graphene. Compared with graphite/GC and bare GC electrodes (both at 0.65 V), the graphene modified electrode displayed wider linear range (0.05–1.4 mM, Fig. 4C inset), lower detection limit (20 μM) and higher sensitivity (12.6 μA mM^{-1}). The analytical performance of graphene/GC electrode is comparable to the reported carbon nanotube modified electrodes [38]. In addition, another attractive feature of the graphene/GC electrode is its stable amperometric NADH response. In a stirred NADH solution (1 mM), the amperometric response of the graphene/GC electrode remained 80% of its initial value after 60 min experiment, while only 45% and 25% are observed at the graphite/GC and bare electrodes respectively, reflecting the better anti-fouling properties during the oxidation process of NADH on the graphene/GC electrode. This feature is very promising for real applications. Compton has reported that at carbon-based electrodes, the dense edge-plane-like defective sites on carbon materials had the effect of resistance to fouling [39]. According to Raman characterization from the literatures [40–42], graphene has more edge-plane-like defective sites compared to graphite, which may play an important role in minimizing passivation effects for NADH oxidation at graphene assembled electrode. The improved electron transfer kinetics of graphene/GC electrode could also contribute to the response stability.

3.4. Amperometric biosensing for ethanol

Because of the better electro-catalytic activity of the graphene/GC electrode towards the oxidation of NADH, an amperometric ethanol biosensor was constructed by integration of ADH with graphene/GC electrode. In an ADH based electrochemical biosensor, ethanol is oxidized to acetaldehyde by a coenzyme, NAD^+ which is necessary to accept electrons from ethanol with the aid of ADH. Concurrently, NAD^+ is reduced to NADH which can be regenerated and recycled at the electrode surface by releasing electrons and proton. The whole process can be illustrated in Fig. 5.

Since the ethanol biosensor response depends on the amount of the immobilized enzyme, various enzyme loadings were prepared by using different concentrations of ADH (4–10 mg mL^{-1}), as shown in Fig. 6A. The ethanol biosensor response increased by raising the concentration of ADH from 4 to 8 mg mL^{-1}. However, a reduced response was obtained with higher enzyme contents of 10 mg mL^{-1}. As a result, 8 mg mL^{-1} ADH was chosen as the opti-

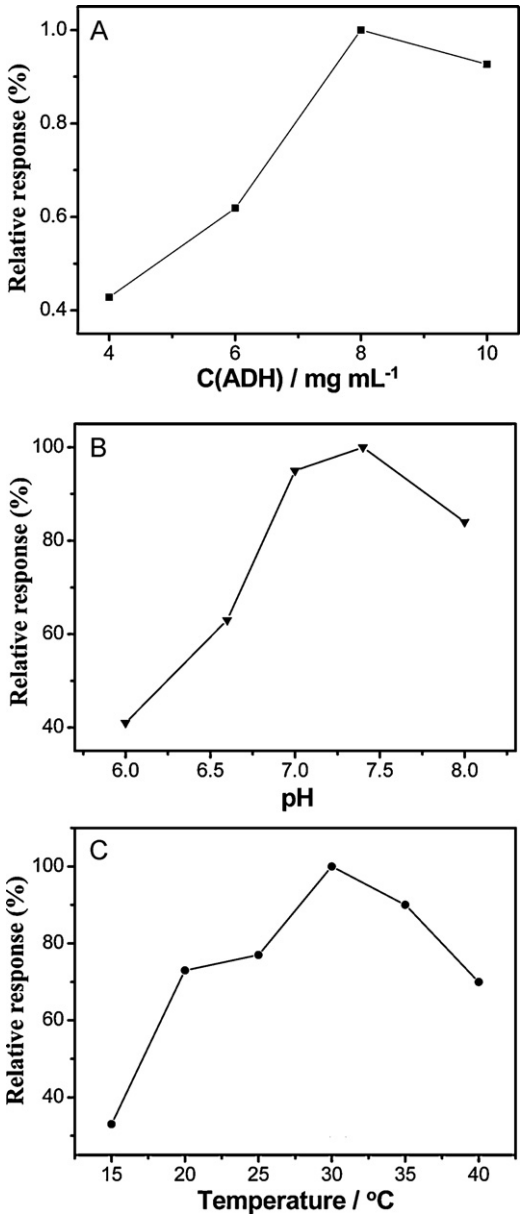

Fig. 6. Amperometric responses of ADH/graphene/GC electrodes at (A) different concentrations of ADH, (B) different pH of PBS solutions and (C) different temperatures for 2 mM ethanol with 5 mM NAD^+ in 0.1 M PBS.

mum enzyme modification for the biosensor fabrication. The effect of pH and temperature on the response of the biosensor was also investigated for 2 mM ethanol with 5 mM NAD^+ (Fig. 6B and C). The prepared biosensors exhibited good behaviors in abroad range of pH values (6.0–8.0) and temperature (15–35 °C). The highest amperometric responses were observed at pH 7.4 and 30 °C, respectively.

Under the optimized condition, the performance of Nafion/ADH/graphene/GC electrode was then evaluated by amperometric response experiment. Fig. 7A shows the steady-state response of Nafion/ADH/graphene/GC electrode with an applied potential of 0.5 V for different additions of ethanol in a stirred 0.1 M pH 7.4 PBS at 30 °C. The response of this biosensor was rather fast and the response time was less than 10 s. The current increased linearly with ethanol concentration over the range from 0.2 to 21.0 mM (Fig. 7B). The detection limit was estimated to be 0.025 mM. Comparison of the results with literature data is given in Table S1. The electrode-to-electrode reproducibility of

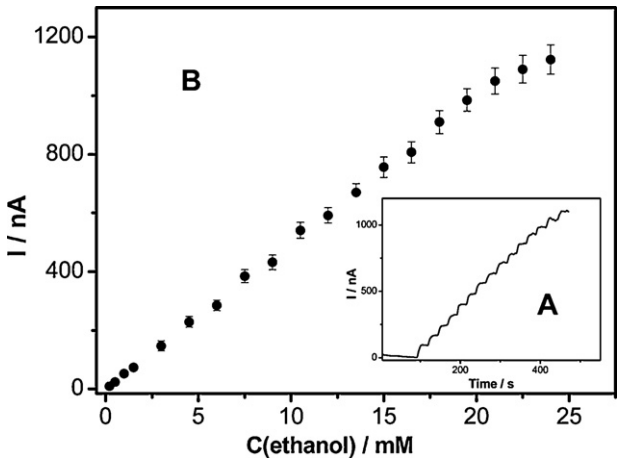

Fig. 7. (A) Current–time curve for Nafion/ADH/graphene/GC (at 0.5 V) electrode with successive addition of ethanol, 1.5 mM each injection in stirred 0.1 M pH 7.4 PBS solution containing 5 mM NAD^+ at 30 °C. (B) Calibration curve for ethanol at Nafion/ADH/graphene/GC electrode. Standard deviation was got from three different electrodes.

this biosensor was determined with the addition of ethanol under 0.5 V using different enzyme electrodes. It shows an acceptable reproducibility with a relative standard derivation (R.S.D.) of less than 5.6%. The stability of the immobilized enzyme electrode was also examined. When not in use, the electrode was stored in 100 mM pH 7.4 PBS at 4 °C in a refrigerator. After two weeks, the amperometric responses towards 5 mM ethanol of the modified electrode remained 89% of its initial value. This high stability can be attributed to the compatibility of the graphene and strongly interaction between enzyme and graphene.

The specificity of Nafion/ADH/graphene/GC was also carried out with other lower molecular weight alcohols and possible interferences, as shown in Fig. 8. It was revealed that under the same condition, the Nafion/ADH/graphene/GC electrodes exhibited little amperometric response to physiological level of interferences and other low molecule weight alcohols. This observation is quite similar with the results obtained from ADH/mesoporous carbon/GC electrode [43]. These results demonstrate that this biosensor has good stability, reproducibility and selectivity, as required for the determination of ethanol.

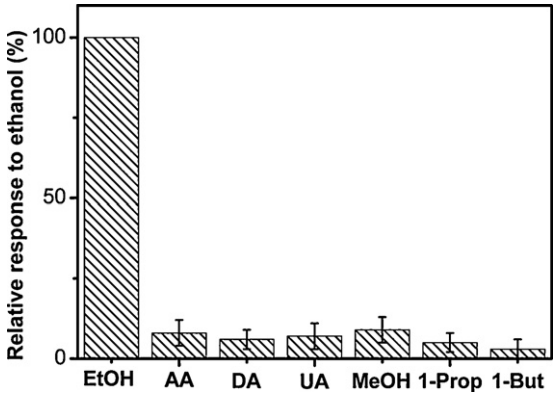

Fig. 8. Comparison of the biosensor response in the presence of low weight alcohols and possible interferences (1 mM ethanol, methanol, 1-propanol and 1-butanol; 0.2 mM ascorbic acid, dopamine and uric acid), the response of 1 mM ethanol as the reference. Measurements were performed at 30 ± 0.5 °C in 0.1 M pH 7.4 PBS with 5 mM NAD^+.

Table 1
Determination and recovery results of ethanol in alcohols by the biosensor.

Sample	Nominal (%, v/v)	Biosensor (%, v/v)	*C* (ethanol)		Recovery (%)	R.S.D. (%)
			Added (mM)	Found (mM)[a]		
White spirit	40.0	38.9 ± 0.6	0.50	0.48	94	4.7
			1.50	1.47	98	5.6
			3.00	3.24	108	3.5
Red wine	12.5	12.8 ± 0.5	0.50	0.52	104	6.1
			1.50	1.43	95	2.8
			3.00	3.10	103	4.9
Beer	3.7	3.9 ± 0.3	0.50	0.51	102	3.8
			1.50	1.60	107	5.2
			3.00	2.80	93	6.4
			3.00	2.80	93	6.4

[a] Average of three measurements.

3.5. Determination of ethanol in alcoholic beverage

In order to evaluate the application of this biosensor, the proposed Nafion/ADH/graphene/GC electrode was tested for the determination of ethanol in three different alcoholic beverages: white spirit, red wine and beer. Each sample was diluted with PBS solution (0.1 M pH 7.4) such that the diluted sample contained approximately 1.5 mM of ethanol in the reaction medium. The results of each beverage obtained at this biosensor were in good agreement with those certified by the manufacturers (Table 1). Furthermore, the recovery measurements for ethanol were also performed in these samples and the results are summarized in Table 1. The application results demonstrate that this biosensor offers an accurate method for the determination of ethanol in real samples.

4. Conclusions

The advantages of graphene sheet modified glass carbon electrodes for the electrochemical biosensing are evaluated. The electrochemical activity of graphene/GC electrode was investigated with electro-active molecular, which show a remarkable increase in the rate of electron transfer compared with graphite/GC and bare GC electrodes. Furthermore, on the basis of well electrocatalytic activity at the graphene/GC electrode towards NADH, ADH was immobilized on the graphene/GC electrode to show faster and selective response with wider linear range and lower detection limit. Moreover, the accurate determination of ethanol in real samples demonstrates the great potential of this proposed biosensor for practical applications. Above all, graphene sheet, with favorable electrochemical activity, may open up a new challenge to explore a range of electrochemical sensing and bio-sensing applications.

Acknowledgements

This work is supported by NSFC 20925517, SKLEAC201101, STCSM (10XD1406000, 09JC1402600) and Shanghai Leading Academic Discipline B109.

Appendix A. Supplementary data

Supplementary data associated with this article can be found, in the online version, at doi:10.1016/j.talanta.2011.05.038.

References

[1] P.A.D. Pereira, E.T.S. Santos, T.D. Ferreira, J.B. de Andrade, Talanta 49 (1999) 245.
[2] A.K. Wanekaya, M. Uematsu, M. Breimer, O.A. Sadik, Sens. Actuators B: Chem. 110 (2005) 41.
[3] G. Lazarova, L. Genova, V. Kostov, Acta Biotechnol. 7 (1987) 97.
[4] P. Tipparat, S. Lapanantnoppakhun, J. Jakmunee, K. Grudpan, Talanta 53 (2001) 1199.
[5] C.X. Cai, K.H. Xue, Y.M. Zhou, H. Yang, Talanta 44 (1997) 339.
[6] A.M. Azevedo, D.M.F. Prazeres, J.M.S. Cabral, L.P. Fonseca, Biosens. Bioelectron. 21 (2005) 235.
[7] M. Zhou, L. Shang, B.L. Li, L.J. Huang, S.J. Dong, Biosens. Bioelectron. 24 (2008) 442.
[8] J. Moiroux, P.J. Elving, Anal. Chem. 50 (1978) 1056.
[9] M.I. Alvarez-Gonzalez, S.A. Saidman, M.J. Lobo-Castanon, A.J. Miranda-Ordieres, P. Tunon-Blanco, Anal. Chem. 72 (2000) 520.
[10] H. Jaegfeldt, T. Kuwana, G. Johansson, J. Am. Chem. Soc. 105 (1983) 1805.
[11] L.D. Zhu, R.L. Yang, X.Y. Jiang, D.X. Yang, Electrochem. Commun. 11 (2009) 530.
[12] A. Salimi, R. Hallaj, M. Ghadermazi, Talanta 65 (2005) 888.
[13] T.R.L.C. Paixao, D. Corbo, M. Bertotti, Anal. Chim. Acta 472 (2002) 123.
[14] C.P. You, X.W. Yan, J.L. Kong, D.Y. Zhao, B.H. Liu, Talanta 83 (2011) 1507.
[15] C.P. You, X. Xu, B.Z. Tian, J.L. Kong, D.Y. Zhao, B.H. Liu, Talanta 78 (2009) 705.
[16] C.P. You, Y. Xuewu, Y. Wang, S. Zhang, J. Kong, D.Y. Zhao, B.H. Liu, Electrochem. Commun. 11 (2009) 227.
[17] M. Musameh, J. Wang, A. Merkoci, Y.H. Lin, Electrochem. Commun. 4 (2002) 743.
[18] Y. Wang, C.P. You, S. Zhang, J.L. Kong, J.L. Marty, D.Y. Zhao, B.H. Liu, Microchim. Acta 167 (2009) 75.
[19] K.S. Novoselov, A.K. Geim, S.V. Morozov, D. Jiang, Y. Zhang, S.V. Dubonos, I.V. Grigorieva, A.A. Firsov, Science 306 (2004) 666.
[20] S. Stankovich, D.A. Dikin, G.H.B. Dommett, K.M. Kohlhaas, E.J. Zimney, E.A. Stach, R.D. Piner, S.T. Nguyen, R.S. Ruoff, Nature 442 (2006) 282.
[21] J.C. Meyer, C.O. Girit, M.F. Crommie, A. Zettl, Nature 454 (2008) 319.
[22] E.K. Athanassiou, F. Krumeich, R.N. Grass, W.J. Stark, Phys. Rev. Lett. 101 (2008) 4.
[23] N. Severin, S. Kirstein, I.M. Sokolov, J.P. Rabe, Nano Lett. 9 (2009) 457.
[24] B.S. Kong, J.X. Geng, H.T. Jung, Chem. Commun. (2009) 2174.
[25] N. Mohanty, V. Berry, Nano Lett. 8 (2008) 4469.
[26] X.L. Zuo, S.J. He, D. Li, C. Peng, Q. Huang, S.P. Song, C.H. Fan, Langmuir 26 (2010) 1936.
[27] M. Zhou, Y.M. Zhai, S.J. Dong, Anal. Chem. 81 (2009) 5603.
[28] C.S. Shan, H.F. Yang, D.X. Han, Q.X. Zhang, A. Ivaska, L. Niu, Biosens. Bioelectron. 25 (2010) 1504.
[29] C. Hontoria-Lucas, A.J. Lopez-Peinado, J.D.D. Lopez-Gonzalez, M.L. Rojas-Cervantes, R.M. Martin-Aranda, Carbon 33 (1995) 1585.
[30] D. Li, M.B. Muller, S. Gilje, R.B. Kaner, G.G. Wallace, Nat. Nanotechnol. 3 (2008) 101.
[31] D.A. Dikin, S. Stankovich, E.J. Zimney, R.D. Piner, G.H.B. Dommett, G. Evmenenko, S.T. Nguyen, R.S. Ruoff, Nature 448 (2007) 457.
[32] W.S. Hummers, R.E. Offeman, J. Am. Chem. Soc. 80 (1958) 1339.
[33] Y.P. Zhang, C.X. Pan, J. Mater. Sci. 46 (2011) 2622.
[34] S. Watcharotone, D.A. Dikin, S. Stankovich, R. Piner, I. Jung, G.H.B. Dommett, G. Evmenenko, S.E. Wu, S.F. Chen, C.P. Liu, S.T. Nguyen, R.S. Ruoff, Nano Lett. 7 (2007) 1888.
[35] S.J. Guo, D. Wen, Y.M. Zhai, S.J. Dong, E.K. Wang, ACS Nano 4 (2010) 3959.
[36] M. Csiszar, A. Szucs, M. Tolgyesi, A. Mechler, J.B. Nagy, M. Novak, J. Electroanal. Chem. 497 (2001) 69.
[37] L.N. Wu, X.J. Zhang, H.X. Ju, Anal. Chem. 79 (2007) 453.
[38] L. Agui, C. Pena-Farfal, P. Yanez-Sedeno, J.M. Pingarron, Electrochim. Acta 52 (2007) 7946.
[39] C.E. Banks, R.G. Compton, Analyst 130 (2005) 1232.
[40] S. Stankovich, D.A. Dikin, R.D. Piner, K.A. Kohlhaas, A. Kleinhammes, Y. Jia, Y. Wu, S.T. Nguyen, R.S. Ruoff, Carbon 45 (2007) 1558.
[41] K.N. Kudin, B. Ozbas, H.C. Schniepp, R.K. Prud'homme, I.A. Aksay, R. Car, Nano Lett. 8 (2008) 36.
[42] A.C. Ferrari, J. Robertson, Phys. Rev. B 61 (2000) 14095.
[43] X.Y. Jiang, L.D. Zhu, D.X. Yang, X.Y. Mao, Y.H. Wu, Electroanalysis 21 (2009) 1617.